

# C80-085

## Biaxial Stress Measurements on Cloth Samples and Bias-Constructed Parachute Models

00008

H.G. Heinrich\*

*University of Minnesota, Minneapolis, Minn.*

Knowledge of canopy stresses is very important in the design of parachutes. Since no suitable sensors were available for measurement of canopy stresses, the Omega sensor was designed for this purpose. The functioning of Omega sensors under biaxial loading of cloth samples was checked and found to be satisfactory. Subsequently, Omega sensors were used to measure the stress of single gores under simulated steady-state conditions using so-called pressure boxes. It was found that bias- and block-constructed gores differ significantly in profile and stress distribution. Also, the measured stresses were higher than the product of differential pressure and bulge radii. The validity of the measurements were proven by measuring the stress of an inflated tube of parachute cloth. The stress distribution of an inflated bias-constructed 4-ft parachute model was established.

### Nomenclature

$D_0$	= nominal diameter
$S$	= distance from vent center
$S^*$	= distance $2S/D_0$
$q$	= dynamic pressure
$\sigma$	= stress, lb/ft
$\sigma^*$	= normalized stress = $\sigma/qD_0$
$\sigma'$	= $\sigma_m/\sigma_{cl}$ dimensionless stress
$\epsilon$	= strain
$d\epsilon/dt$	= strain rate

### Subscripts

$c$	= circumferential
$cl$	= calculated
$ccl$	= circumferential calculated
$r$	= radial
$ss$	= steady-state
$m$	= measured

### I. Introduction

CALCULATIONS and measurements of the stress in parachute canopies has been the subject of earlier investigations. The recent summary of these studies is shown in Ref. 1. The stress measurements were carried out by means of Omega sensors, which development and functioning was described earlier.<sup>2,3,4</sup> While the sensor was developed and first used at the University of Minnesota, two other agencies also have recently used Omega sensors and have reported satisfactory functioning.<sup>5,6</sup> Of particular importance is the finding at the Research Institute at Braunschweig, Germany, that the sensors worked satisfactorily up to strain rates  $d\epsilon/dt$  of 500% per s.<sup>6</sup> At Minnesota, similar tests could be carried out only up to 100% per s.<sup>4</sup> Also, Ref. 6 states that the eigenfrequency of the sensors under investigation was approximately 1.70 kHz, which is sufficiently higher than any known opening frequency of parachutes. Figure 1 illustrates the principle of the Omega sensor. Its sensing elements are a curved metal beam and electric strain gages. To avoid transfer of bending moments from nonrigid surfaces to the sensor, the

ends of the curved beam are glued to the structure by means of cloth tabs. Under the open side of the beam is a slot in the cloth, and the stress is transferred across the slot by the sensor.

The net effect of a possible interference with the natural stress flux is eliminated by means of calibrating the Omega sensor versus an applied stress after it is attached to the cloth.

Since the stress-strain characteristics of nylon and other synthetic materials not only have a nonlinear stress-strain relationship, but also have a strong hysteresis, Omega sensors were also tested under loading and unloading conditions.<sup>7</sup> Figure 2 shows the difference in strain for a loading and unloading cycle, the hysteresis, and the sensor signal versus the stress caused by an externally applied load. One notices that the signal remains linear in spite of a very pronounced hysteresis, and this indicates that the Omega sensor measures stress independent of strain. This independence is very important for using the sensor for stress measurements of parachutes. This is true since during the inflation the force between parachute and suspended load varies considerably with respect to time, and the stress in the parachute cloth must vary in a somewhat related manner.

### II. Biaxial Stress Measurements on Individual Cloth Samples

Previous publications (see Refs. 1-5) are related to uniaxial stress measurements of block-constructed parachute models. However, many parachutes are bias-constructed, and for these parachutes one cannot really speak of radial and circumferential stress. Since the gores are not homogeneous sheets but compositions of tightly arranged and interwoven yarns, held together by friction, one must assume that the tension forces will primarily travel along the yarns, and the terms of radial and circumferential stresses are somewhat hypothetical ideas. Therefore, and in view of the status of the theoretical stress analyses, a true picture of the stress distribution of a bias-constructed parachute can presently be obtained only by experimental studies. The Omega sensor has been very successful in connection with block-constructed parachute canopies, but no results are known for bias-constructed parachute canopies and biaxial loading of parachute cloth.

Therefore, a test stand was built in which cruciform cloth samples could be biaxially loaded by means of a centrally arranged weight and four individual load carrying cables. To assure equal loading of the arms, each cable had a spring scale and a turn buckle for correcting unequal extension of the cloth sample in warp and fill. Figures 3 and 4 show the

Presented as Paper 79-0425 at the AIAA 6th Aerodynamic Decelerator & Balloon Technology Conference, Houston, Texas, March 5-7, 1979; submitted March 29, 1979; revision received Aug. 6, 1979. Copyright © American Institute of Aeronautics and Astronautics, Inc., 1979. All rights reserved.

Index category: Deceleration Systems.

\*Professor, Department of Aerospace Engineering and Mechanics. Fellow AIAA. Deceased.

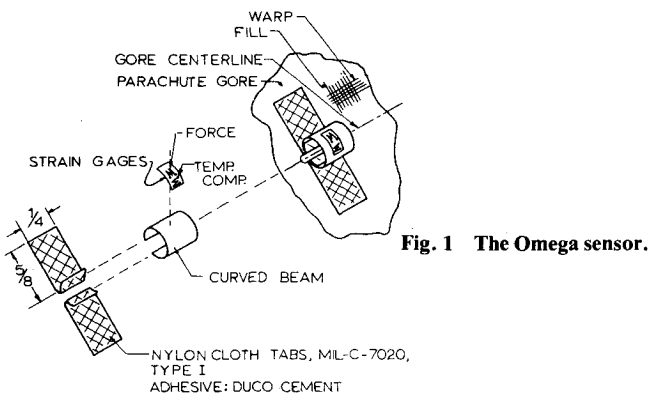


Fig. 1 The Omega sensor.

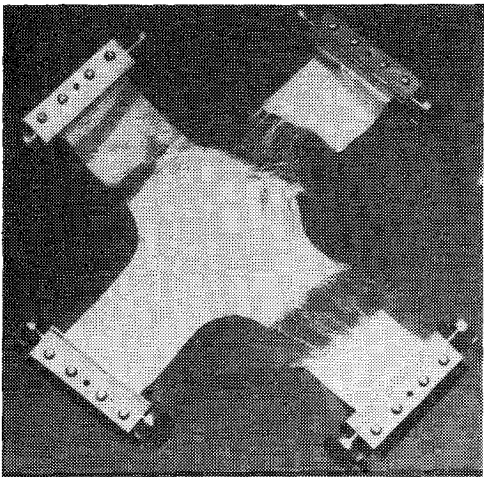


Fig. 4 Cloth sample destroyed in biaxial loading.

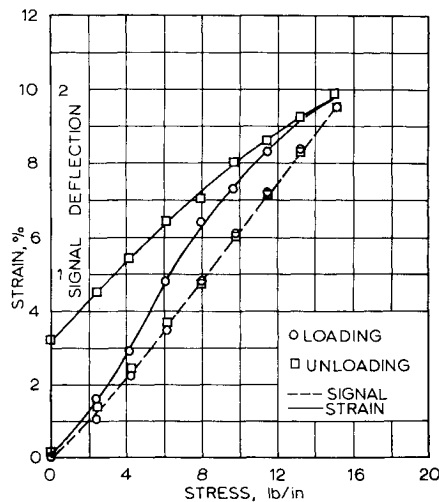


Fig. 2 Constant sensor output, independent of hysteresis.

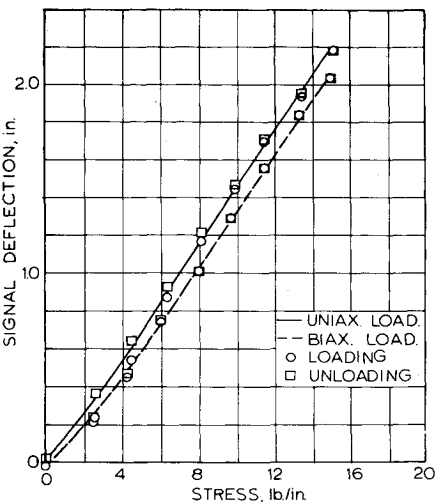


Fig. 5 Sensor calibration under uniaxial and biaxial loading.

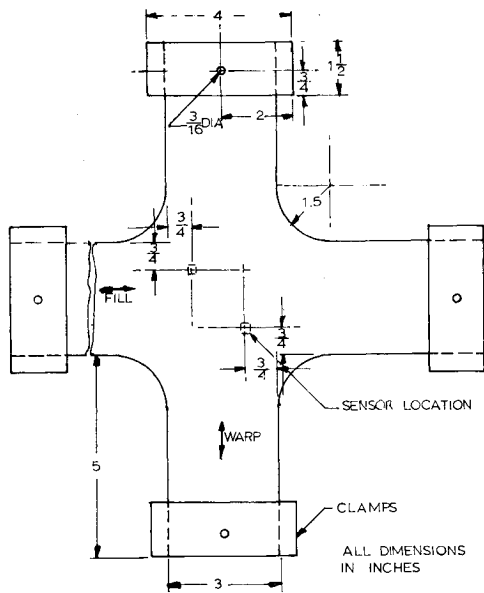


Fig. 3 Cloth sample for biaxial loading, MIL C7020-Type 1.

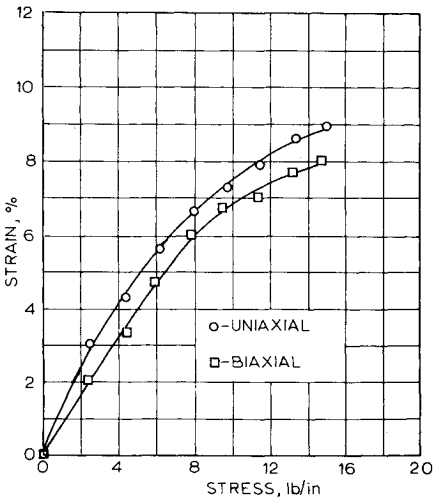


Fig. 6 Stress-strain diagram under uniaxial and biaxial loading.

dimensions of the cloth sample and a sample after loading to the ultimate.

Before biaxial loading of the samples, the sensors were calibrated by uniaxial loading in warp and fill, and only those which showed satisfactory linearity were used for further tests. Also, one notices in Fig. 5 that the calibration of the sensors differs slightly for uniaxial and biaxial loading. It was generally found that the difference was between 3 and 7%,

and for actual stress measurements under the biaxial loading condition, this may have to be considered.

Another result of uniaxial and biaxial loadings was (see Fig. 6) that the nylon cloth was less elastic when biaxially loaded. Also, it was noticed that the cloth did not recover to its original stress-strain characteristic even after 24 h of relaxation. However, the signal-stress relationship remained

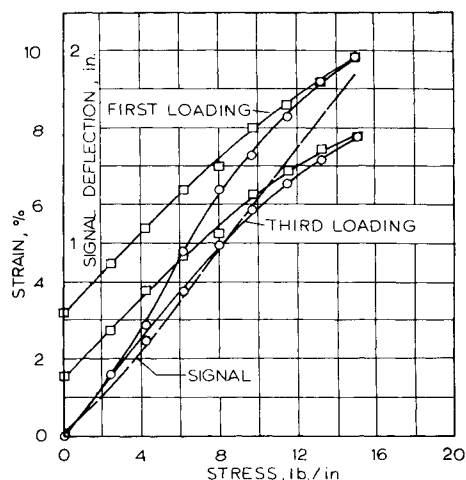


Fig. 7 Stress-strain and signal deflection at first and third loading.

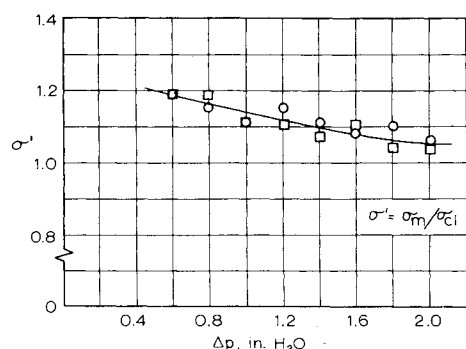


Fig. 8 Circumferential stress of a circular cloth cylinder.

unchanged as can be seen in Fig. 7. Therefore, this hysteresis effect, if it occurs in parachutes during inflation or at steady-state would not affect the accuracy of measurements.

All described measurements and calibrations were made with cloth samples under straight pull conditions. In order to check the usefulness of the sensor for measuring stress on a curved parachute gore, a cylinder was manufactured with rigid endplates and a cylindrical surface of parachute nylon cloth. The cylinder had a 4-in. diam and a 20-ft. length. The warp yarns were arranged in the direction of the longitudinal axis and the fill yarns perpendicular to it. An Omega sensor was fastened to the surface in the direction of the fill yarns, and measured the circumferential stress when the cylinder was inflated with compressed air.

The cylinder was chosen because the circumferential stress should be approximately  $\sigma_{cl} = \Delta p \cdot r$ , and the value  $\sigma^* = \sigma_m / \sigma_{cl}$  is a good indication of the accuracy of measurements. Figure 8 shows the results, and one notices that at higher pressures values close to unity were obtained. During the tests, it was also observed that the longitudinal yarns were extended, and the cylinder assumed somewhat the form of a barrel with enlarged diameters in the middle section. This deformation develops additional circumferential stress, and is probably the reason that more circumferential stress was measured than predicted by the simple formula stated earlier. Applying a longitudinal force reduced the circumferential stress. The bulge radius  $r$ , which is contained in the stress formula, was measured at the middle for a differential pressure of one inch of  $H_2O$ . Considering the somewhat complicated stress measurements and the elastic features of the cloth, one can accept the relatively good agreement between measured and calculated stress, particularly at the higher differential pressures, as proof that the Omega sensor will give satisfactory values for parachute stress measurements on curved cloth surfaces.

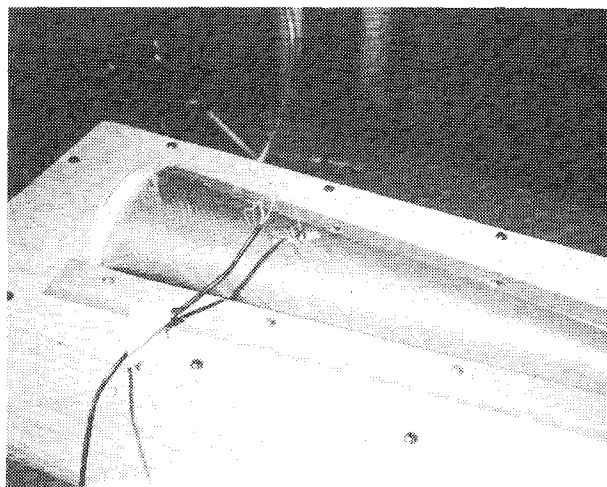


Fig. 9 Straight pressure box with parachute gore.

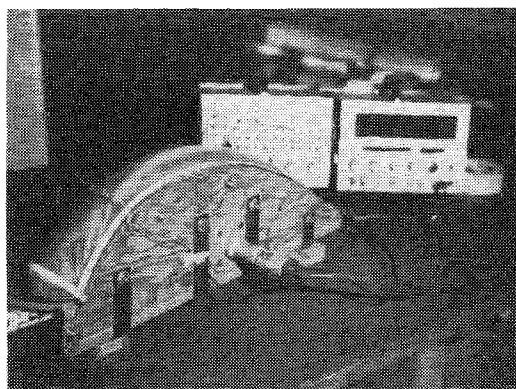


Fig. 10 Curved pressure box with parachute gore.

### III. Stress Measurements on Isolated Canopy Gores

Biaxial stress measurements on inflated parachute gores are a new technique, and it was thought that it would be advantageous to measure the material stress of single gores before attempting to measure biaxial stress on inflated parachute models. Therefore, so-called pressure boxes were built in which isolated gores can be studied. An inflated parachute gore is actually a two-dimensionally curved shell, and for stress measurements one must consider the gore structure, block- or bias-constructed. Two types of pressure boxes, straight and curved, were used (see Figs. 9 and 10).

#### A. Tests with the Straight Pressure Box

In the straight pressure box, the inflated gore forms the surface of a straight cone for which the calculation of the circumferential stress in homogeneous material is relatively well-known. Therefore, the idea was to measure the stress of sample gores in the straight pressure box and compare them with stresses calculated by the formula  $\sigma_{cl} = \Delta p \cdot r$ . The underlying concept of these tests was that if in these cases the measured and calculated stresses agree satisfactorily, then the measured stresses in a curved box must also be right.

The assumption that the stress in a parachute gore would be like the one of a homogeneous conical surface would best be matched by a block-constructed gore. In a block construction, one may assume as first approximation that the yarns arranged perpendicular to the gore centerline carry the circumferential force between adjacent suspension lines. Therefore, the first tests were made with block-constructed gores. The results of these tests are summarized in Fig. 11, where  $\sigma$  is the ratio of the measured stress, and  $\sigma_m$  divided by the calculated stress  $\sigma_{cl} = \Delta p \cdot r$ . The radius  $r$  was measured at a differential pressure of one inch of  $H_2O$ .

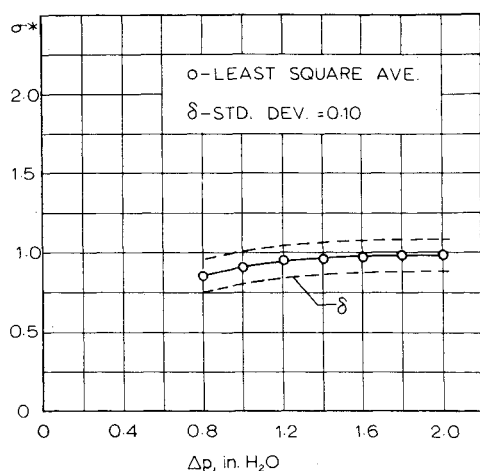


Fig. 11 Circumferential stress at  $s^* = 0$  of a block-constructed gore in the straight pressure box ( $\sigma_l = \sigma_m / \sigma_{cl}$ ).

Figure 11 indicated that the measured and calculated stresses agree satisfactorily in the higher pressure range. The variation of the stress versus the pressure is probably caused by characteristics of the nonhomogeneous nylon cloth and the internal friction of the yarns.

Considering the cloth characteristics and the experimental method, the measured and calculated stresses agree satisfactorily.

In view of the test results, one may conclude that in a straight pressure box the yarns between adjacent suspension lines carry practically the entire circumferential force.

In a bias-constructed gore the fill and warp yarns, which intersect the centerline under 45 deg, must also carry the force between adjacent suspension lines. Also, in order to measure the respective stress, the Omega sensor must be placed in the direction of the yarns, which is under 45 deg to the gore centerline (see Fig. 9). In order to measure the stress in fill and warp, different gores were used since two sensors close to each other seem to affect the natural stress flux too much.

A number of tests were made, and the results were repeatable. However, the stresses measured in the directions of fill and warp were considerably larger than the 45 deg component of the circumferential stress calculated from  $\sigma_{cl} = \Delta p \cdot r$ , where  $r$  is the bulge radius between adjacent suspension lines intersecting the gore centerline under 90 deg. For comparison, another theoretical stress was calculated from  $\sigma_{cl} = \Delta p \cdot r'$ . Here  $r'$  is the radius of a circular arc which intersects the gore centerline under an angle of 45 deg at the location of the sensor, while the related cord is the distance between the points where the arc intersects the adjacent suspension lines. The circular arc is an approximation of the radius or curvature of the elementary surface of individual yarns. The real curvature varies, of course, from left to right due to the conical surface of the gore.

The related radii were determined by measuring the inflated gore, and the calculated stress  $\sigma_{cl} = \Delta p \cdot r'$  was used to normalize the measured stress.

The results of these tests are summarized in Fig. 12. One notices that the normalized stresses approach unity, which means that the assumption that the diagonally directed force is carried along the yarns in fill and warp direction, and that the arc of these yarns in the formula  $\sigma_{cl} = \Delta p \cdot r'$  is an acceptable term. However, it means also that the old assumption of

$$\sigma_{fill} = \sigma_{warp} = 1/2 \sigma_{cl} / \cos 45 \text{ deg} \quad (1)$$

with  $\sigma_{cl} = \Delta p \cdot r$  is erroneous.

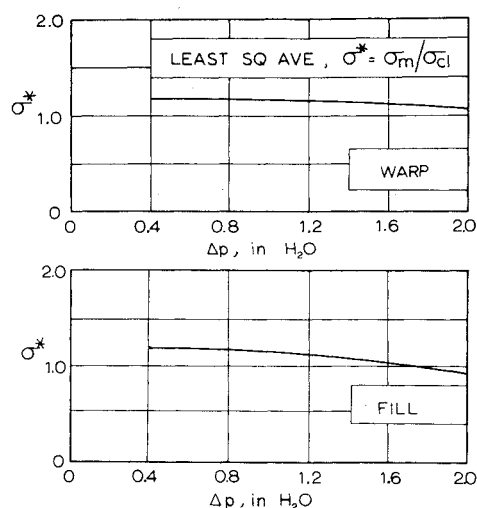


Fig. 12 Stress in bias-constructed gores at  $s^* = 0.8$  in the straight pressure box.

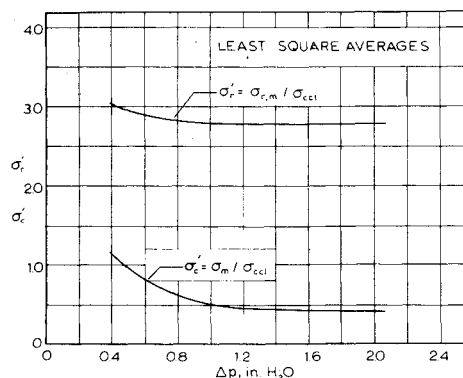


Fig. 13 Circumferential and radial stress of block-constructed gore in curved pressure box,  $s^* = 0.8$ .

The deviation from unity at lower pressures is probably caused by the nonlinear extension of the cloth.

Summarizing the results of the tests with the gores in the straight pressure box, one may conclude that:

- 1) The measured values represent real stress at the centerlines of the gores.
- 2) For block-constructed gores, the circumferential stress is a function of the bulge radius intersecting the gore centerline perpendicularly.
- 3) In bias-constructed gores, the actual stress is close to a calculated stress, using in the stress formula, the radius of a circular arc which intersects adjacent suspension lines and the gore centerline under 45 deg.

#### B. Tests in the Curved Pressure Box

Arranging the sample gores in a curved pressure box introduced a second curvature, and one has to expect that in block- as well as in bias-constructed gores, all stress will change.

In the straight pressure box, the radial stress in the block-constructed gore was negligible at  $s^* = 0.8$ , and it did not appear to be significant at other radii. In the curved pressure box, the radial stress is approximately six times higher than the circumferential stress (see Fig. 13). This is surprising, however, a number of tests were made and the dispersion of the individual results was relatively small.

These results indicate that the double curvature of the canopy profile induces strong radial stresses. Somewhat similar results were already reported from experiments with flexible block-constructed parachute models,<sup>1,3</sup> and these pressure box results seem to be very significant. However, on

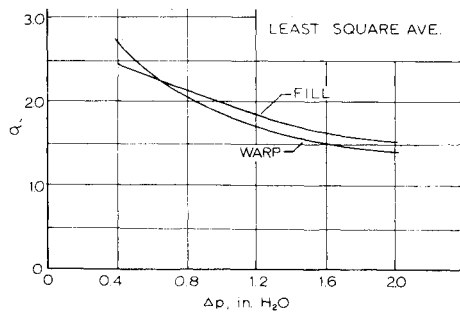


Fig. 14 Stress in bias-constructed gores in curved pressure box,  $s^* = 0.8$ .

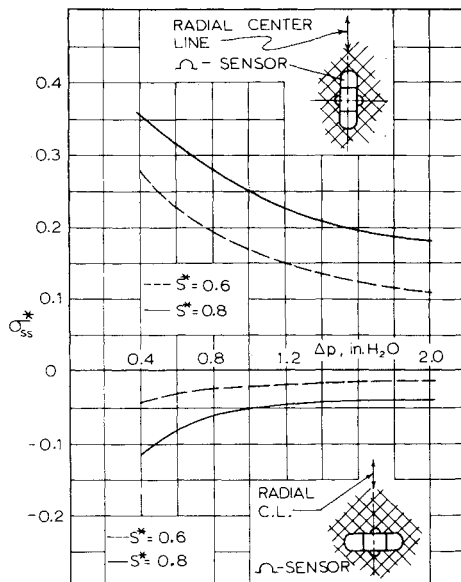


Fig. 15 Stress in bias-constructed gore measured in radial and circumferential direction (averaged values).

the parachute model the difference between radial and circumferential stresses was smaller, and one may assume that the gore profile in the pressure box is not identical to the profile of a gore on an inflated parachute.

It should also be mentioned that the skirt of all simulated gores was tested in the same pressure box, and the results are summarized in Fig. 14. One notices that over the pressure range the fill and warp yarns are almost equally loaded. The variation of the stress with the pressure is again probably caused by the elongation of the longer yarns of the bias construction which leads to smaller bulge radii with increasing pressure. Comparing the stresses in block- and bias-constructed gores, one notices the much more uniform loading in the bias-constructed gore, which indicates more efficient use of the cloth.

In all pressure boxes, measurements of the stress decline with increasing pressure. As mentioned before, this may be caused by the elongation of the nylon cloth under tension which leads to smaller bulge radii, and in turn to relatively lower stress. Also, the figures may be distorted somewhat because the calculated stress, which is used for normalization, is based on a bulge radius established at a differential pressure of one inch of water.

Since the existing theories operate with composite values, tests were made in which bias-cut gores were equipped with radially and circumferentially arranged sensors and inflated in the curved pressure box. These tests and their results are illustrated in Fig. 15. The positive as well as the negative were repeatable, however, a physical identification of these stresses could not be given. Therefore, further efforts to interpret or

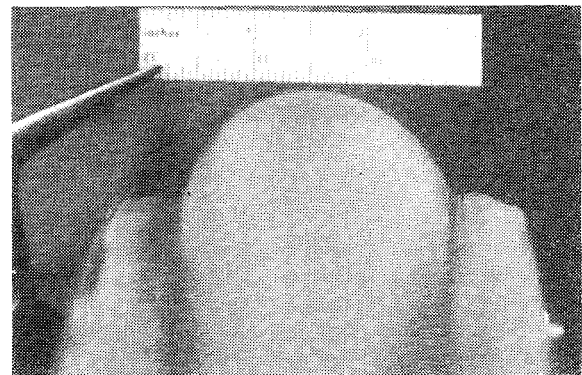
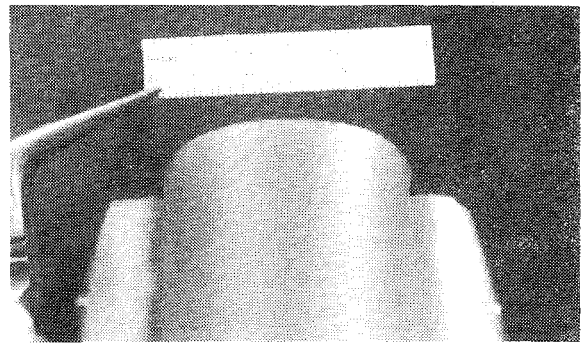


Fig. 16 Typical profiles of block- and bias-constructed gores in curved pressure box.

analyze this type of measurement did not seem to be justified. In all tests with the curved pressure box, the stress was considerably different than stresses predicted by the published theoretical analyses.

Since in the simple cases of the cloth cylinder and the block-constructed gores in the straight box the calculated and measured stresses are approximately equal, one may conclude that the measured stress for the block- and bias-constructed gores in the curved pressure box indicates, within experimental limits, correct values of the actually existing stress. Then one must admit that for block- and bias-constructed gores, the conventional methods of stress calculation give erroneous results.

#### IV. Bulge Radii of Block- and Bias-Constructed Gores

In the tests in the curved pressure box, one noticed also that the bulge profiles of the block- and bias-constructed parachutes were quite different (see Fig. 16). Both pictures were taken at differential pressure of two inches of water column. The strongly flattened profile of the block-constructed gore is obviously caused by strong radial stresses, which in turn lowers the circumferential stress. Both effects were also seen in the stress measurements.

Block-constructed parachutes do not look as flat as the gore in the pressure box, and one may conclude that the profile of block-constructed parachutes is different from the profile of the curved pressure box.

The curvature of the pressure box is identical to the profile of real bias-constructed parachutes,<sup>8</sup> and one may assume that the simulated single- and bias-constructed gores are curved in all respects similar to actual parachute gores. Therefore, the stress measurements on bias-constructed gores reflects closely the stress of actual gores, whereas the measurements of block-constructed gores are probably not fully representative for block-constructed parachutes.

However, in view of all model tests, there are good reasons to believe that the stress distribution of bias-constructed parachutes is more favorable than the stress in block-constructed parachutes.

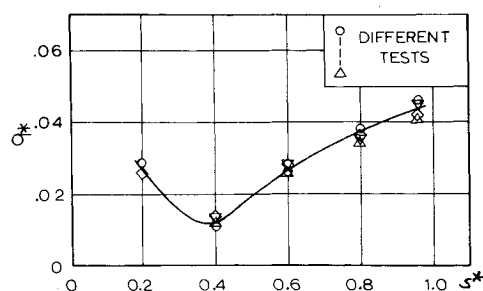


Fig. 17 Stress distribution of a 4-ft solid flat parachute at steady-state, warp direction cloth MIL C7020-I, 9 = 7.1 lb/ft<sup>2</sup>.

### V. Stress Distribution of a Bias-Constructed Parachute Model

After these preparatory tests, stress measurements were made with two 4-ft bias-constructed solid flat circular parachute models with 28 gores. Five sensors were arranged at the gore centerline in warp or fill direction at the distances from the apex of  $s^* = 0.2, 0.4, 0.6, 0.8$ , and  $0.96$ .

The results of tests with the sensors arranged in warp direction are shown in Fig. 17. The characteristic of the curve is somewhat like a 5-ft Ringslot parachute,<sup>1</sup> however, the pressure values are about twice as high. The data points were repeatable, and the presented curve seems to be realistic. Because of the importance of the stress problem, further studies should be made.

Tests to establish the stress distribution in fill were not completed when this paper went to print. However, in view of Fig. 14, the stress distribution in fill direction is not expected to be significantly different.

### Acknowledgments

This study was sponsored by the U.S. Air Force under Contract E33615-C-0020 and by funds from the University of Minnesota. R. Schultz and D.R. Reynolds, students of the University of Minnesota, participated in the accomplishment of the research objectives.

### References

- <sup>1</sup>Heinrich, H.G. and Saari, D.D., "Parachute Canopy Stress Measurements at Steady-State and During Inflation," *Journal of Aircraft*, Vol. 15, Aug. 1978, pp. 534-539.
- <sup>2</sup>Heinrich, H.G. and Noreen, R.A., "Stress Measurements on Inflated Model Parachutes," Air Force Flight Dynamics Lab., AFFDL-TR-72-43, Feb. 1972.
- <sup>3</sup>Heinrich, H.G. and Noreen, R.A., "Experimental Stress Analysis on Inflated Model Parachutes," AIAA 4th Aerodynamic Deceleration Systems Conference, Palm Springs, Calif., May 21-23, 1973.
- <sup>4</sup>Heinrich, H.G. and Noreen, R.A., "Functioning of the Omega Sensor on Textile Samples under High-Loading Rates," Air Force Flight Dynamics Lab., AFFDL-TR-74-78, Sept. 1974.
- <sup>5</sup>Wagner, Peggy M., "Experimental Measurement of Parachute Canopy Stress during Inflation," AFFDL-TR-78-53, May 1978.
- <sup>6</sup>Braun, G. and Doherr, K.F., "Experimentelle Untersuchung von Omega-Aufnehmern zur Messung der Spannungen in flexiblen Fallschirmkappen," 154-78115, Braunschweig, Germany, Aug. 1978.
- <sup>7</sup>Heinrich, H.G., "On the Status of Experimental Stress Analysis of Parachute Canopies," *Proceedings of the 16th SAFE Symposium*, San Diego, Calif., Oct. 1978.
- <sup>8</sup>Berndt, R.J., "Experimental Determination of Parameters for the Calculation of Parachute Filling Times," *Jahrbuch des Wissenschaftlichen Gesellschaft fuer Luft-und Raumfahrt, E.V. (WGLR)*, Friedr. Vieweg and Sohn Braunschweig, Germany, 1964, pp. 299-316.

## From the AIAA Progress in Astronautics and Aeronautics Series . . .

### REMOTE SENSING OF EARTH FROM SPACE: ROLE OF "SMART SENSORS"—v. 67

Edited by Roger A. Breckenridge, NASA Langley Research Center

The technology of remote sensing of Earth from orbiting spacecraft has advanced rapidly from the time two decades ago when the first Earth satellites returned simple radio transmissions and simple photographic information to Earth receivers. The advance has been largely the result of greatly improved detection sensitivity, signal discrimination, and response time of the sensors, as well as the introduction of new and diverse sensors for different physical and chemical functions. But the systems for such remote sensing have until now remained essentially unaltered: raw signals are radioed to ground receivers where the electrical quantities are recorded, converted, zero-adjusted, computed, and tabulated by specially designed electronic apparatus and large main-frame computers. The recent emergence of efficient detector arrays, microprocessors, integrated electronics, and specialized computer circuitry has sparked a revolution in sensor system technology, the so-called smart sensor. By incorporating many or all of the processing functions within the sensor device itself, a smart sensor can, with greater versatility, extract much more useful information from the received physical signals than a simple sensor, and it can handle a much larger volume of data. Smart sensor systems are expected to find application for remote data collection not only in spacecraft but in terrestrial systems as well, in order to circumvent the cumbersome methods associated with limited on-site sensing.

505 pp., 6 × 9, illus., \$22.00 Mem., \$42.50 List

TO ORDER WRITE: Publications Dept., AIAA, 1290 Avenue of the Americas, New York, N. Y. 10019